Observation of surf zone wave transformation using LiDAR

Matthew Harry[a], Hong Zhang[ab*], Charles Lemckert[cb], Gildas Colleter[d], Chris Blenkinsopp[d]

a. School of Engineering and Built Environment, Griffith University, Gold Coast Campus, QLD 4222, Australia
b. Griffith Centre for Coastal Management, Cities Research Institute, Griffith University, QLD4222, Australia
c. Built Environment and Design, University of Canberra, Bruce, ACT, 2617, Australia
d. Jeremy Benn Pacific, Brisbane, Qld 4004, Australia
e. Department of Architecture and Civil Engineering, University of Bath, Claverton Down, Bath BA2 7AY, UK

***Corresponding Author:** Hong Zhang; Postal Address: School of Engineering and Built Environment, Griffith University, Gold Coast Campus, QLD 4222, Australia ; Tel + 61 7 55529015; Email address: hong.zhang@griffith.edu.au

Matthew Harry; Email address: matthew.harry87@gmail.com

Charles Lemckert; Email address: Charles.Lemckert@canberra.edu.au

Gildas Colleter; Email address: Gildas.Colleter@jbpacific.com.au

Chris Blenkinsopp; Email address: c.blenkinsopp@bath.ac.uk

Abstract

The use of LiDAR as an alternative to an array of in-situ instruments for water elevation measurement, specifically in the surf zone, is covered in detail. This paper outlines the advances in remote sensing of the coastal environment and provide both laboratory and field observations obtained through the application of LIDAR scanning devices. The results of this paper show a good correlation between LiDAR and pressure transducer measurements of water elevation in both a wave flume and within the surf zone (mean coefficient of determination of 0.76 and 0.89 respectively). The water surface reflectivity of the study area needs to be maximised in order for the LiDAR to provide suitable measurements, therefore a method of seeding in the wave flume is described. Points to consider for the setup of the LiDAR instrument in both the laboratory and the field are discussed, as well as the influence that wave parameters such as wave height and wave period have on the quality of results. Free surface elevation data across the spatial and temporal domain can be obtained with LiDAR and used for a wide range of wave analyses.

Key words

LiDAR; Remote sensing; Wave measurement; Wave flume; Surf zone

1. Introduction

The measurement of wave properties in the surf-zone is a research field that constantly innovates as technological capacity increases. Various instruments have been used to observe the many hydrodynamic processes intrinsic to the surf-zone. In-situ devices have been developed for the laboratory and the field to measure properties such as flow velocity, turbulence and surface elevation. In-situ devices are in physical contact with the water body and generally need to be placed as an array if more than one position is to be studied. Whether it is practical to place an array of instruments in-situ depends on the coverage required and the process to be observed. For example, pressure transducers are commonly deployed in the surf zone due to their relative ease of installation and their ability to estimate surface wave heights derived from linear wave theory (Bishop & Donelan, 1987).

Remote sensing techniques, of which there are many, allow instrumentation to be conveniently located near a water body with no direct interaction with the water body, resulting in measurements and observations that do not interfere with hydrodynamic processes. For example, water elevation measurements at a fixed position can be obtained using acoustic or

LiDAR gauges. A time series of water elevation is measured by these instruments at a distance from the surface of the water, usually from directly above (Irish et al., 2001). Innovative techniques have been devised to measure wave properties such as using light projection (Kouyi et al., 2003), 3-D PIV (Du & Li, 2009), colour block projection (Watanabe et al., 2011), and in the field, RADAR for breaking wave detection (Haller & Lyzenga, 2003). Preliminary research on shallow angle LiDAR indicated that sea surface elevations could be measured remotely and across the spatial domain (Horwood et al., 2005). Good agreement between surface measurements from a LiDAR and array of ultrasonic altimeters in the swash zone has shown that the technology can be utilized in the surf zone for cross-shore flow velocity measurements (Blenkinsopp et al., 2010).

The total crest elevation, shape and transformation of waves in the surf zone can be difficult to measure due to the dynamic nature of the water surface. Problems also arise in the post-breaking phase of wave propagation where the presence of air bubbles can affect the accuracy of some measurement techniques. In addition, breakers in the field are more difficult to study as a number of measurement techniques used in wave flumes are impractical to install or operate in the surf zone. The present study outlines the use of LiDAR for free-surface measurements, including points to consider to maximise quality of results, as well as presenting both experimental data from wave flume tests and field data collected from the surf zone.

2. LiDAR for water profile measurement

This paper will focus on the use of LiDAR for 2D profile measurements at a fixed point only due to practicality and the nature of the target surface; however as technology improves, inexpensive high frequency 3D scanners will no doubt become feasible. There are a number of commercially available LiDAR systems capable of providing detailed measurements of 2D profiles from manufacturers such as Leica, Riegl and Sick AG.

Scanning instrumentation either uses the time-of-flight principle or phase based optics to determine target distances. The instrument used in the experiments discussed in this paper uses time-of-flight in which the instrument emits a laser pulse towards the target object and subsequently detects the reflected light. The range of the object from the LiDAR system is determined by the time it takes for the transmitted pulse to travel to the object and reflect back to the sensor on the instrument. This will be recorded as a single point in space in relation to the point of origin at the LiDAR.

There are a number of factors that can influence the success of utilising LiDAR technology for dynamic free-surface profile measurements. These factors are inherent of the technology and therefore specific conditions need to be met in order to maximize the quality of results obtained from LiDAR instrumentation. These are, surface reflectivity which depends on the physical properties of the intended target, and lesser factors that include the angle of incidence, range and environmental conditions. Specular reflection is the direct reflection of light at an angle equal to the angle of incidence, whereas diffuse reflection is the scattering of light in many directions and at different intensities. LiDAR has the greatest chance of detecting diffuse reflections as the probability of a single, or multiple, return echo from the target direction is higher. Imperfections or roughness of the surface of the target object scatter the light and increase the chances of this occurring.

These airborne LiDAR systems use a combination of two different laser wavelengths to distinguish the water surface from the sea bed in order to determine the bathymetric elevation (Guenther et al., 2000). This can be achieved due to the difference in surface reflectivity of both bodies which is closely related to the physical properties of the materials (although not entirely due to this). The surface reflectivity in any individual study needs to be considered if LiDAR is to be used for free-surface water profile measurements, and this needs to be maintained otherwise there will be a loss of suitable data (Harry et. al, 2012). This applies to both experimental and field studies. However, the restrictions and advantages of the use of LiDAR in either situation are quite different. In a controlled experimental setup, say in a laboratory, the source of water would generally be from drinking water supplies or recycled water. Clarity of the water prevents a strong surface reflection signal and the laser pulse will more than likely pass through and reflect from the surface of the water body container. To overcome this problem various techniques can be used to change the optical properties of the water such as spreading a buoyant material across the surface or adding particulate matter to the water body (Blenkinsopp et al., 2012). In the surf zone phenomena such as biological matter, surface ripples, foam and bubbles all contribute to an increase in surface reflectivity compared to calmer water bodies and to experimental setups (Belmont, 2007).

The output of LiDAR systems are generally comprised of a point cloud or a matrix of data points, with 3D coordinates and time being the primary parameters. The point cloud can be validated against known reference points such as fixed objects within the instruments line-of-sight, or specifically for this study, data obtained from independent surface tracking

instruments. If validation of the point cloud data is not performed then a seemingly complete data set assumed to be representative of measured water surface may not be accurate. If a laser pulse penetrates the water surface and reaches another target past this point (such as the beach slope in a wave flume) a reflection is possible and will be detected by the LiDAR system as a valid data point. The laser pulse will undergo refraction as it passes from one medium to another that will in turn lengthen the travel time for that pulse resulting in a longer calculated range than if the water body was not there. This does assist in the identification of data points that are not of the water surface as there will be a noticeable difference between these points and the expected surface position. However if the data set is not checked adequately these points may go unnoticed. For this study each of these issues were addressed through control of the experiments or post processing of the collected data.

3. Methodology

For both the flume and the field studies the LiDAR used was a LMS511-20100 PRO Laser Measurement Sensor produced by SICK. The instrument uses a Class 1 laser with a wavelength of 895-915nm. The instrument has a maximum field of view of 190° with an angular resolution and scanning frequency that are dependent on each other. The minimum angular relocation of the instrument is 0.1667° and the maximum scanning frequency is 100Hz. A balance between resolution and frequency was preferred with the LiDAR operating at 0.25°@35Hz. The instrument has a scanning range of up to 80m and can filter data points using up to 5 echoes from a single laser pulse. Output from the scanner is in the form of scan angle and the corresponding distance to the reflection of the laser pulse determined by the time-of-flight principle.

3.1. Flume measurements

A laboratory experiment was conducted using a LiDAR and array of pressure transducers (PT) in a 2D glass-walled wave flume at the Griffith School of Engineering, Griffith University, Gold Coast. The setup is illustrated in Figure 1 and includes a summary of simulated surf conditions. The effective test section dimensions from the end of the beach slope up to the wave paddle are 12 m long, 0.45 m wide and 0.8 m deep. A HR Wallingford piston-type Wave Generation System was used to generate waves in the flume. The beach slope was constructed to scaled dimensions of irregular bathymetry representative of a Gold Coast beach including a single submerged berm. Table 1 summarises the experiments conducted and their associated parameters. A total of 4 wave heights and 3 wave periods were used in combination.

The LiDAR was mounted centrally above the wave flume approximately 1m from the flume bed and 1.5m (x =1.5 m) along the flume from the beach end extent of the bathymetry. This position ensures that the front face of the waves were within the LiDAR line of sight.

A total of ten Druck PTX 1830 pressure transducers sampling at 10 Hz were installed along the flume centreline. Their positions along the flume were chosen to maximise the coverage of all wave transformation stages and thus the interval is irregular. The data from each PT was calibrated using the linear method and subsequently the pressure transfer function of Eq. 1 and Eq. 2 was applied (Nielsen, 1989). As defined in these equations, a local approximation method is used to smooth the signal.

$$A\left(\frac{z}{d}\right) = 0.67 + \frac{0.34z}{d} \qquad \text{Eq. 1}$$

$$\eta_n = \frac{p_n}{\rho g} exp\left[A\left(\frac{z}{d}\right)\frac{-p_{n-M} + 2p_n - p_{n+M}}{p_n g(M\delta)^2}\left(d + \frac{p_n}{\rho g} - z\right)\right] \qquad \text{Eq. 2}$$

where p is the measured pressure, ρ is the water density, g is the gravitational constant, z is the instrument depth, η is the free surface elevation and d is the total water depth. Furthermore, smoothing of the data is achieved by selecting the M^{th} neighbor of the n^{th} point rather than the nearest neighbour. Calibration parameters for each PT were calculated independently prior to correction for pressure attenuation.

Sphericel Grade 60P18, which is a white glass hollow microsphere (appearance of a powder) with a bulk density of 0.32 g/cc and an approximate particle size of 20 μm, was dispersed throughout the water to act as reflective particulate matter. Without the addition of Sphericel the water did not have adequate surface reflectivity to enable measurements using LiDAR. Although the material is buoyant and when mixed will remain suspended, the particles would build up on the porous surface of the foam bathymetry sections as wave activity increased. Therefore regular top up and mixing of the material was required. The quantity of Spherical used to provide the initial reflective conditions was approximately 0.15 g/L.

In addition to the instruments detailed above, high-speed video was taken at the approximate breaking point and was used to provide a secondary source for validation of the LiDAR data. High-speed video was obtained with use of a HiSpec 1 High-Speed Camera produced Fastec Imaging. Video was taken with a resolution of 1280x780 pixels at a speed of 100 frames per

second (fps). It captures high spatial resolution data rather than point measurements, which is the real method to confirm that the LIDAR captures wave shape. The camera was supported on a tripod located approximately 1.8m away perpendicular from the glass flume wall. A 25 mm F1.4 lens was attached to the camera to give an effective span at the flume of approximately 1.3m. Reference points to assist in image correction were taken from 0.1m horizontally spaced markings on the lower section of the flume wall. In addition, string was attached to the flume wall at 0.4m horizontal and 0.2m vertical spacing forming a relatively sparse grid over the flume wall.

3.2. Field measurements

The aims of the field study were to trial the performance of a LiDAR system for coastal water elevation measurements and to obtain wave crest and breaker height data in the surf zone. In the field many of the LiDAR performance factors will be influential and therefore site selection is important. For this study two locations were trialled where the LiDAR could be mounted above the surf zone due to the limited range of the instrument. The locations were at the Tweed River Entrance Sand Bypassing Project jetty and the Gold Coast Seaway Sand Bypass Jetty. Both jetties are aligned perpendicular to their respective beach and are essentially aligned eastwards from the shore (Tweed jetty is closer to bearing ENE as shown in Figure 2).

At the Seaway Jetty the mounting position for the LiDAR was on the southern side of the jetty supported by a cantilever beam attached to a maintenance platform. At the Tweed jetty the LiDAR was mounted on the Northern side of the jetty cantilevered from a handrail. INW Aquistar PTX2 pressure transducers running at 8 Hz were also deployed from the jetty and placed at the sea bed. Calibration and correction for pressure attenuation was achieved with the same methods as the Druck sensors used in the laboratory. Due to the relatively deeper water in the field, a higher value for parameter M in Eq. 2 was used. A schematic of the general setup of the instrumentation is shown in Figure 3. Due to setup the position on the jetty being over 50m from shore, the PT's were lowered from the jetty and weighed down with concrete blocks. Data obtained from the Department of Environment and Science, Queensland Government, Gold Coast waverider buoy shows that significant wave height over the two fieldwork days ranged from 1 - 1.6 m and an average wave period of 5.75 sec. High flow velocities in the surf zone made it difficult to stabilise multiple PT's and so only one PT was used and stabilised directly below the LiDAR (Figure 4). Surface reflectivity in the field was adequate during the study period due to the conditions experienced in the surf zone and therefore no surface

treatment was necessary. Further trials are needed to determine under what range of conditions the LiDAR technology can be effectively employed.

Bathymetry measurements, as seen in Figure 5, were taken at the Tweed jetty allowing for all instruments and surf zone parameters to be referenced to the Australian Height Datum (AHD). Bathymetry was measured with a weighted rope at 5 m intervals spanning 70 m in total. The elevation of the jetty deck is 8 mAHD the LiDAR was positioned at 9 mAHD.

4. Results and discussion

Data collected from the flume experiment and from the field work are both used to investigate the effectiveness of LiDAR for free-surface measurements, nevertheless the two studies are presented separately below. Data processing of the LiDAR and PT measurements are the same for both studies. The LiDAR data is initially converted into Cartesian coordinates resulting in 2D elevation data along a plane parallel to the direction of wave propagation.

LiDAR acquired profiles of the water surface can be either spatially or temporally interpolated depending on the use of the data, however in most cases interpolation of both domains is necessary. Data points are recorded at a specific angular resolution prior to processing resulting in a spatially non-uniform distribution of data point along the scanned profile. Therefore, if a time-series of water elevation at any location is desired, spatial interpolation is required to achieve a continuous, and regularly spaced, water surface profile. Although there are non-uniform to uniform mapping techniques, such as those suggested by Belmont (2007), simple interpolation was deemed suitable for this study. Temporal interpolation of the LiDAR profile at a fixed point may be necessary for validation against data obtained from insitu devices. Noise reduction can be implemented if required. However, for these studies where the return signal was generally strong, interpolation techniques were adequate.

4.1. Regular wave profiles

Spatial interpolation of each LiDAR measured wave profile was performed prior to any other processing allowing for a relatively simple comparison with PT results. This also provides a chance to ensure that the data is time synchronised and that the reference levels are the same. The time series water elevation for three locations prior to temporal interpolation is presented in Figure 6 and it is evident that noise is present in both the LiDAR and PT data. In this initial run it is noticeable that with spatial interpolation only the noise levels are of a greater magnitude in the PT9 device being at the deepest point for this comparison. Nevertheless, there is good

agreement between the LiDAR and PT furthest from the shore at PT9 and the elevation peaks are of the same magnitude. For the data presented in Figure 6, the location of PT7 coincided with the point of maximum wave shoaling and the initiation of breaking. A 5 Hz filter was applied to the PT measurements and a comparison between this and the LiDAR time series elevations correlated well except for some variation between the maximum peaks. These observations were also observed using the unfiltered PT data, therefore to reduce complexity in the data processing the unfiltered data was used for the study. The LiDAR measured a peak elevation near the breaking point of approximately 15 mm higher than the PT (approximately 30% higher). Due to the nature of pressure transducer technology and the use of linear wave theory, the free surface of wave crests at the break point and of aerated water columns can be underestimated and this is the case in this figure. It is likely that aeration affects the PT measurements in the swash and post-breaking zones and that discrepancies due to use of the pressure transfer function affect the pre-breaking zones. In contrast, LiDAR can detect the free surface as long as the reflection intensity is maintained. Therefore, it is evident that the maximum peak elevations measured by the LiDAR at PT7 are likely not to be an overestimation and that subsequent processing of the wave series, such as smoothing by temporal interpolation, will provide a conservative value for the maximum wave crest elevation compared to the raw data. In aerated sections of the flume where a foamy surface is detected by the LiDAR there is uncertainty as to whether this is the actual water surface, however this would also depend on the definition used for the water surface (e.g. whether the outermost foamy matter is considered the surface or not). Matching both the LiDAR and PT data is in some ways ambiguous due to the interpretation required to define a water surface that is common to both instruments. This does not however mean that a comparison is undeserved; the aim of the study is to check controlled flume measurements with those from the field and if consistency is achieved the comparison is valid. Also noticeable at PT7 is a lowering of the LiDAR measured water level and this is due to changes in the reflectivity of the entire water body over time. PT4 exhibits an even greater apparent loss of water level and this highlights the importance on monitoring the surface properties of the water while using LiDAR. The phenomenon is due to the dispersion of the seeding material, as well as some build up of the particles on the bathymetry and loss of the material around the sides of the bathymetry. Reduction in the concentration of the material then allows penetration of the LiDAR pulses into the water body at until a strong reflection is detected. Monitoring of the concentration of the seeding material for this study was done by eye. Loss of concentration is a case by case problem depending on the wave parameters and flume setup unique to each study. Subsequent

runs used greater concentrations and any trends were corrected for concurrent with applying temporal interpolation. An alternative explanation is that multiple reflections off the water surface, resulting in an apparent increase in range, could account for the discrepancy. Without a comprehensive analysis of different seeding materials and concentrations the main contributor to the error is uncertain, however observations from this study have shown that regular maintenance of a high concentration seeding material can reduce the error.

Determining the performance of the LiDAR instrument in comparison with each PT is an important point of analysis due to the effect of variation in angle of incidence and potential shadowing in the line-of-sight. A total of 9 different combinations of wave height, wave period and position along the flume are presented as a series of scatter plots in Figure 7. Each plot places 1 minute of data (spatially and temporally interpolated LiDAR data and spatial interpolated PT data) from both instruments against each other according to the parameters set in Table 2. Observations of each plot in conjunction with Table 2 allows for the discussion of a number of parameter combinations between the runs. Runs 1 to 3 show the relationship between LiDAR and PT elevations using fixed wave parameters over the course of wave transformation through three locations. Minimum and maximum wave elevation changes between each location are immediately observable. For Run 9 where waves have not yet broken correlation is apparent between the two data sets, however the scatter is noticeably spread out. In part this is due to the larger surface fluctuations, however the effect of incidence angle from the LiDAR instrument helps push the data points away from the 1:1 line due to the instrument limitations. Successful data points at the wave crest are less frequent under some conditions (for example at a further distance from LiDAR and longer wave periods) due to the spatial and temporal interpolation that is required to align with a corresponding PT data point. The high angle of incidence at the wave crest increases the chance of an edge reflection that would still be recorded by the instrument. Correlation for Run 2 is the best of this selection and there is a distinct separation between the high concentration of points at the crest and the trough (Nonetheless, this can be observed in certain degrees for all runs). The standard deviation of the LiDAR-PT difference is the lowest in Run 2 (similarly in Run 1, however this is well after the wave has broken) at just under 3.5 mm equaling just over 6.5% of the wave height at PT7. The first three runs exhibit expected scatter clouds for each stage of wave transformation and the only implication for the use of LiDAR is that range understandably increases the error. For Runs 4 to 9 the location was fixed at PT9 and either the wave height was changed, or the wave period. Runs 4 to 6 start at a period of 4 s and halve for each run. The most significant

observation is the lack of data points through the mid-wave height elevation for Run 6 and to a lesser extent Run 5. The greatest density of points is in the lower half of Run 6 due to the steepness of the wave profile. The steep wave face results in a rapid change in elevation reducing the chance of a LiDAR data point being recorded at the specific cross-shore position, however more importantly, wave steepness increases the amount of shadowing occurring blocking the lee side of the wave from the line-of-sight. Therefore, the elevation distribution of LiDAR data points at an arbitrary location along the free surface profile depends on the wave period. Also of note is the difference between Run 3 and Run 9 which, as it happens, also shows a change in the period only and follows this conclusion by exhibiting a lower density of data points above the SWL for a shorter wave period. Finally, Runs 7 to 9 show the results from changes in wave height only and the only major difference between the three scatter plots is the maximum and minimum elevations reached, which is expected, and therefore the spread of points to cover this changing envelope. The effect of wave height on the distribution of correlating data points was not as significant as the wave period was for this experiment, however if the waves were high enough then shadowing could be a factor. An example of shadowing is given in Figure 8 where a single profile scan of Run 6 is plotted. The wave steepness and LiDAR height above the water determine whether shadowing will influence the percentage of each wave profile that is in the line-of-sight. This is not a problem for regular waves such as those produced in the flume experiment, however for an irregular wave climate there would be a percentage of waves in the spectrum with low wave heights that are shadowed by the preceding wave.

Collating all of the data from the 12 possible combinations of wave period and wave height for a water level of 0.17 m allows for a conclusion of the overall correlation of the LiDAR and PT data. The scatter plot for these combinations is presented in Figure 9 and is the result of 12 minutes recording time totaling almost 20,000 data points. Linear regression results in a coefficient of determination, R^2, of 0.76 and a standard deviation, σ, of 5.02 mm, and from an observation of the plot it can be seen that the defining feature of the data is the bias towards overestimation of elevation measured from the LiDAR at higher wave heights. The reason for the digression from the 1:1 line was indicated in Figure 6 with wave peaks near the breaking point exhibiting features more favorable for detection with the LiDAR system. Validation of LiDAR surface profile data is relatively easy to achieve for any experimental study as long as the secondary measurement devices, such as pressure transducers, are located at some point

along the profile. The scanned free surface profile can be processed to provide time series elevation data at any point within the devices range.

The phase-dependent error was calculated and used to compare the time series measured from both LiDAR and PT. This comparison used the data from all runs and was segregated into their respective wave periods (1, 2 and 4 seconds). From these three groups an indicative (and normalized) time series was produced for plotting purposes and placed on each time series was the standard deviation error bars at period-dependent intervals. The standard deviation was derived from the statistical analysis of all corresponding LiDAR and PT data with a matching wave period and time interval. In Figure10 the three wave period groups are displayed. It can be seen that the error is not dependent on elevation even though the 1 and 2 second wave period data indicate that may be the case. Rather it is the rate of change of elevation that has resulted in the highest errors between the LiDAR and PT data which are greater in magnitude due to discrepancies in syncronisation and wave attenuation correction. Taking this into consideration it can be concluded that when the wave face and wave crest pass the point of measurement the correlation between both instruments is affected. Although undertaking the analysis of the phase-dependent disagreement provided further evidence of the differences between LiDAR and PT, understanding whether either instrument is more accurate than the other was still in some way ambiguous.

To support the statements on the accuracy of LiDAR, independent of the PT results, high-speed video was taken of what was the predominant breaker zone (x = 5 - 6.25 m). Image processing of the video involved the use of tilt, perspective and distortion corrections as well as contrast alterations to assist in edge detection. The water surface was derived from the boundary between the water body (as seeding provided a cloudy appearance to the water) and the black background. In Figure 11, a comparison between the LiDAR and video data for two particular times is shown. The figure shows the typical accuracy of the water surface profile measured by the LiDAR in comparison with the spatially referenced and corrected video images. The two instances of the profile data show pre-breaking and post-breaking. In either case it can be observed that the LiDAR profile matches the video profile for the majority the common measured data points. There is good correlation especially at the wave face. Although the length of the profile is not complete in both data sets presented in Figure 11, comparable agreement is observable over successive wave profiles providing evidence of consistent coverage over the study domain. The coverage was not complete at each individual profile due

to seeding and illumination limitations as discussed. Considering the challenges in setting up ideal experimental conditions for both the LiDAR and video instrumentation the results are significant. Inaccuracies in the LiDAR measurements include potential surface penetration whereas the video data assumes a perfectly 2-D generated wave is captured at the flume wall. From the analysis of the video measurements it can be concluded that the accuracy of the LiDAR as determined from the PT comparison is valid.

One use of the LiDAR profile scanning ability is the measurement of maximum wave crests in the surf zone. A maximum wave crest profile can be hard to obtain in flume experiment, just as with any surf zone characteristic that would require an array of devices for it to be measured. LiDAR data that has been processed can provide reliable, spatially expansive data within the limits of the power of the device. As can be seen in Figure 12 the LiDAR can provide ample data for the construction of wave crest profiles. The three wave profiles in Figure 12 are of various initial wave heights and have been spatially and temporally interpolated. Indeed, the flume setup does not provide ideal deep water waves so shoaling is immediately observed. The breaking point for each profile is easily observable with the larger waves breaking earlier as expected. The only anomaly in the wave profiles is the peak at 5.5 m along the flume for the highest wave. Following the breaking point a significant splash is observed and in turn this affects the wave crest profile. This could possibly be eliminated with the use of a more complex algorithm that ignores large vertical velocities, however for this comparison the absolute maximum is used. These maximum crest profiles can be easily derived from the LiDAR scans and highlight the use of spatial interpolation, whereas the time series analysis above is more reliant on temporal interpolation. Either way the LiDAR data proves to be highly versatile lending itself to different types of analysis.

It is shown that measurements of breaking waves using LiDAR can yield highly detailed data of water surface topography. The advantage of this technique is that there is significantly less post processing required whilst still remaining easy to set up and operate. The LiDAR device is therefore suitable for deployment in the field as the difficulties and limitations of other techniques that confine the measurements in the laboratory do not apply, for instance with cross-sectional video of the surf zone and PIV systems.

4.2. Surf zone measurements

Field work at the Tweed jetty demonstrated consistent performance using the SICK LiDAR. The pressure transducers were attached to a flat bottom weight and lowered into the water from

a jetty. For validation purposes, the Tweed jetty results are presented as the conditions were favourable. The offshore wave conditions at the attempted time of data collection were H_s 1m and T_z 4.5s (measured within 10km of the study site). At the Tweed jetty it was possible to stabilise a single pressure transducer in line with the LiDAR, however this was at a distance away from the jetty of around 5 meters and therefore not directly below the scanning profile. The offshore wave conditions at the time of data collection at were H_s 1.25 m and T_z 5.75 s (measured from over 30 km of the study site). The depth of the sensor was measured with an approximation based on the measured bathymetry and the height of the base. The mean water level measured by the LiDAR and the PT was also used to correct the elevation values. The propagating waves were essentially 2D, yet influence from three-dimensionality cannot be excluded in the surf zone, particularly adjacent to a jetty structure. Initial comparison between the LiDAR and PT data (both temporally interpolated) shows good agreement and similar characteristics to the flume experiment comparisons. A selection of approximately 2 minutes of this data can be seen in Figure 13. Although the general elevation changes are matched quite well, the LiDAR data can exhibit higher crest peaks compared to the PT peaks. However, there is a better match for the peaks in the field than what was measured in the flume. Also of note in Figure 13 is the comparatively lower trough elevation from the PT data. This is a result of the pressure attenuation correction equations over compensating for the non-linearity of the waves. However, compared to the flume results the equations are more suited to the field setup and conditions, and this is evident in the relatively good correlation of the general wave shape including the wave crest. Inaccuracies may also be introduced due to dynamic pressure fluctuations from currents. Another aspect of the free surface that the LiDAR instrument excels in measuring is the higher frequency elevation fluctuations which are lost from PT measurements with an increase in depth.

Linear regression of over 35,000 data points from both LiDAR and PT results in a coefficient of determination, R^2, of 0.89 and a standard deviation, σ, of 47 mm. The scatter plot in Figure 14 shows that there is good agreement between the two devices, however the trends seen here are similar to those that are experienced in the wave flume. There is a high density of points near the 1:1 line with overestimation of surface elevation by the LiDAR noticeable for some records above the SWL. This measurement of the wave peaks is congruent to the results observed in the flume, however the density along the 1:1 line is relatively constant leading to the conclusion that shadowing is not as influential in this field setup. If the LiDAR was mounted at a lower position, say on the shore, then the shadowing effect would become a factor.

Observations of the scanned field wave profiles (similar to that of Figure 8) indicated that shadowing was not a significant factor, and in fact the LiDAR range was the limiting factor. If an instrument with a longer range was used then shadowing would have been more likely due to a smaller possible angle of incidence with the mean water level. As mentioned, the PT was mounted directly below the LiDAR and so the scatter plot is valid for this location only. Further seaward the scanned profile is well defined, however there are points where splash back from waves impacting the jetty piles fell into the line of sight and were detected by the instrument. At these locations it is required that these spurious results are filtered out so as to not influence the measurement of the actual free surface. This should be considered when selecting a site for positioning of the LiDAR - in this case there were raked piles which stepped out from the Northern side of the jetty -- so that external influences in the free surface can be minimised. In the present study, the indirect method of pressure senor measurement has been adopted successfully. However, comparing LiDAR technology to direct measurement techniques such as automated trinocular stereo imaging system would be of great interest and improve results, which will be implemented in future study.

The large data set can be used to analyse the maximum and minimum wave heights through the study domain, and how the water level is vertically distributed over time in a water column. Just over an hour of profile scans is included in the density plot in Figure 15. This figure shows a normalized density plot of all data points recorded by the LiDAR. The study domain of approximately 60 m was split into 1 m wide slices to be individually analysed. The vertical distribution of data points in each slice is then determined and visualized in the plot. This method allows a more efficient use of the raw data, rather than first spatially and temporally interpolating the data as was the case with the validation above. This allows for a simple determination of the water surface elevation envelope over the specified time period. From observations on site it was noted that all waves entering the domain were unbroken and the shore side of the domain an unbroken wave rarely passed, therefore a relatively wide section of the surf zone is captured in the domain. Checking for sensitivity against the PT results, the 1% and 99% passing profiles are a good preliminary indication of crest and trough maximas through the surf zone. The effect of splash back and false reflections is eliminated using this method allowing for quick results prior to noise removal and interpolation. Further research using this analysis method should aim to capture wave data from multiple sources distributed across the study area which would allow for the verification of suitable passing profiles. Further research into LiDAR for wave profile measurement would also involve the individual time

series analysis at an arbitrary interval across the entire profile. The complexity of an analysis can be scaled depending on the requirements of any study that uses LiDAR measured data.

4.3. LiDAR performance

As discussed in section 2, the primary performance factor for LiDAR is surface reflectivity. In the flume the conditions need to be monitored to ensure that the surface reflectivity is maintained, otherwise the LiDAR may instead penetrate the surface resulting in discrepancies while defining the profile (as seen in Figure 6). Nevertheless, although the physical properties of the surface are important a number of secondary factors also contribute to the overall quality of results and must be taken into consideration. Due to the nature of attempting to measure a water surface with LiDAR, managing these secondary factors can become crucial. The secondary factors need to be avoided or used to an advantage in order to maximise the effective surface reflectivity of what is an already difficult medium to work with.

Angle of incidence effects can be negligible if the surface reflectivity returns a strong signal, however if the experimental setup or conditions in the field are not ideal then effects can produce erroneous points. The return pulse intensity will be lower if the angle of incidence is high due to the elongation of the pulse beam width at the surface. It is also know that the signal is always stronger from a perpendicular surface because, while there is scattering most of the light is reflected back toward the Lidar, and when the angle of incidence is high, most light is reflected toward the horizon. A dynamic free-surface being measured over time will present a number of angles of incidence, therefore at each discrete mirror angle a change in reflection intensity will be detected over time. At extreme angles of incidence, such as at the crest of a wave measured from LiDAR at a low elevation, spurious data points may be recorded due to the pulse beam striking the edge of the surface. In the flume the most unreliable data from the LiDAR was from directly beneath the instrument. At this point the beam encountered the surface approximately perpendicularly and passed through further than at any other angle. This was due to the incident angle as well as inadequate seeding, particularly at the beach end of the flume where loss of particulate matter was more apparent.

Range can also be considered and this also depends on the specifications of each LiDAR system. For the field measurements of this study the surface conditions were favourable and therefore the range was limited only by the power of the instrument. In the field other factors that need to be considered are the environmental conditions at the time of the study. Humidity, precipitation and sea spray are minor factors that may alter the return signal slightly. Most

LiDAR systems filter data points depending on the return intensity (and can distinguish between multiple echoes) and so these factors should not significantly affect results under most weather conditions. For both the laboratory and field studies the LiDAR operated in fine conditions and so the quality and quantity of data was maximised.

5. Conclusion

This paper has detailed a number of factors that will influence the results of water elevation measurements obtained with LiDAR technology in both the laboratory and in the field. A method of seeding for flume experiments is described with observations suggesting a high level of control over the flume setup is required to reduce leakage of the material which may lead to a reduction in concentration of the material. Comparisons between the LiDAR and pressure transducer data from the flume and surf zone show a good correlation with a mean coefficient of determination of 0.76 and 0.89 respectively. Depending on the LiDAR position, wave shadowing is a geometric line-of-sight problem and the result of a combination of wave height and wave period and can affect the percentage of the wave profile that can be measured. However the most significant factor is the reflectivity of the water surface, which in the field was only tested under relatively consistent conditions. As conditions in the surf zone change it is expected that the number of a measured data points in a profile will change as well. With that said, the accuracy of an individual wave profile is supported when compared with video data in the flume. Based on the findings of this study the use of LiDAR for wave profile measurement in the laboratory and the field can be an accurate and efficient method if the water surface is suitably reflective for the sensors of instrument that is to be employed.

6. Acknowledgements

I would like to acknowledge the Australian Postgraduate Award scholarship, which has supported the research leading to this paper. Also I would like to acknowledge the UNSW Water Research Laboratory for providing access to the LiDAR instrumentation and Coastal Impacts Unit, Department of Environment and Science, Queensland Government for providing the waverider buoy data.

7. References

Belmont, M. R. (2007). Application of non-uniform to uniform data mapping to: Shallow angle LIDAR with the introduction of independent variable techniques. *Signal Processing, 87*(10), 2461-2472. doi: http://dx.doi.org/10.1016/j.sigpro.2007.04.005

Bishop, C. T., & Donelan, M. A. (1987). Measuring waves with pressure transducers. *Coastal Engineering, 11*(4), 309-328. doi: http://dx.doi.org/10.1016/0378-3839(87)90031-7

Blenkinsopp, C. E., Mole, M. A., Turner, I. L., & Peirson, W. L. (2010). Measurements of the time-varying free-surface profile across the swash zone obtained using an industrial LIDAR. *Coastal Engineering, 57*(11–12), 1059-1065. doi: http://dx.doi.org/10.1016/j.coastaleng.2010.07.001

Blenkinsopp, C. E., Turner, I. L., Allis, M. J., Peirson, W. L., & Garden, L. E. (2012). Application of LiDAR technology for measurement of time-varying free-surface profiles in a laboratory wave flume. *Coastal Engineering, 68*(0), 1-5. doi: http://dx.doi.org/10.1016/j.coastaleng.2012.04.006

Brodie, K.L., Raubenheimer, B., Elgar, S., Slocum, R.K., McNinch, J.E. (2015). Lidar and Pressure Measurements of Inner-Surfzone Waves and Setup. *Journal of Atmospheric and Oceanic Technology*,, 32, 1945–1959

Costa, B. M., Battista, T. A., & Pittman, S. J. (2009). Comparative evaluation of airborne LiDAR and ship-based multibeam SoNAR bathymetry and intensity for mapping coral reef ecosystems. *Remote Sensing of Environment, 113*(5), 1082-1100. doi: http://dx.doi.org/10.1016/j.rse.2009.01.015

Du, H., & Li, M.-g. (2009). The study for particle image velocimetry system based on binocular vision. *Measurement, 42*(4), 619-627. doi: http://dx.doi.org/10.1016/j.measurement.2008.10.011

Guenther, G. C., Cunningham, A. G., LaRocque, P. E., & Reid, D. J. (2000). *Meeting the accuracy challenge in airborne lidar bathymetry.* Paper presented at the Proc. 20th EARSeL Symposium: Workshop on LIDARRemote Sensing of Land and Sea.

Haller, M. C., & Lyzenga, D. R. (2003). Comparison of radar and video observations of shallow water breaking waves. *Geoscience and Remote Sensing, IEEE Transactions on, 41*(4), 832-844. doi: 10.1109/tgrs.2003.810695

Harry, M., Zhang, H., & Colleter, G. (2012). Remotely sensed data for wave profile analysis. *Coastal Engineering Proceedings; No 33 (2012): Proceedings of 33rd Conference on Coastal Engineering, Santander, Spain, 2012*.

Harry, M., Zhang, H., Lemckert, C., Colleter, G. (2014). Measurement of the Scale Effect on Breaking Waves. *The 11th ISOPE Pacific/Asia offshore mechanics symposium*, Shanghai, China, October 12-16, 2014.

Horwood, J. M. K., Thurley, R. W. F., Belmont, M. R., & Baker, J. (2005, 20-23 June 2005). *Shallow angle LIDAR for wave measurement.* Paper presented at the Oceans 2005 - Europe.

Irish, J., Wozencraft, J., & Cunningham, A. (2001). Water Wave Measurement with Lidar from a Fixed Platform *Coastal Dynamics '01* (pp. 998-1006): American Society of Civil Engineers.

Kouyi, G. L., Vazquez, J., & Poulet, J. B. (2003). 3D free surface measurement and numerical modelling of flows in storm overflows. *Flow Measurement and Instrumentation, 14*(3), 79-87. doi: http://dx.doi.org/10.1016/S0955-5986(03)00011-6

Martins, K., Blenkinsopp, C.E., Zang, J. (2016). Monitoring individual wave characteristics in the inner surf with a 2-dimensional laser scanner (LiDAR), *Journal of Sensors*, 1-11. doi:10.1155/2016/7965431.

Nielsen, P. (1989). Analysis of Natural Waves by Local Approximations. *Journal of Waterway, Port, Coastal, and Ocean Engineering, 115*(3), 384-396. doi: doi:10.1061/(ASCE)0733-950X(1989)115:3(384)

Watanabe, Y., Mitobe, Y., & Oshima, K. (2011). AN IMAGING TECHNIQUE FOR MEASURING WAVE SURFACE SHAPES. *Coastal Engineering Journal, 53*(04), 549-565. doi: 10.1142/s0578563411002458

1 Table 1 Combination of Wavemaker parameters contributing to a total of 12 runs

Wave height (m)	0.075, 0.1, 0.125, 0.15
Wave period (s)	1, 2, 4

2

3

Table 2 Details for all runs displayed in Figure 9 including coefficient of determination and standard deviation of the difference between LiDAR and PT data points

Run	PT	H (m)	T (s)	R^2	σ (mm)
1	4	0.125	4	0.73	3.44
2	7	0.125	4	0.90	3.47
3	9	0.125	4	0.83	6.61
4	9	0.075	4	0.78	4.29
5	9	0.075	2	0.71	5.03
6	9	0.075	1	0.69	4.17
7	9	0.075	2	0.71	5.03
8	9	0.1	2	0.80	7.34
9	9	0.125	2	0.78	8.15

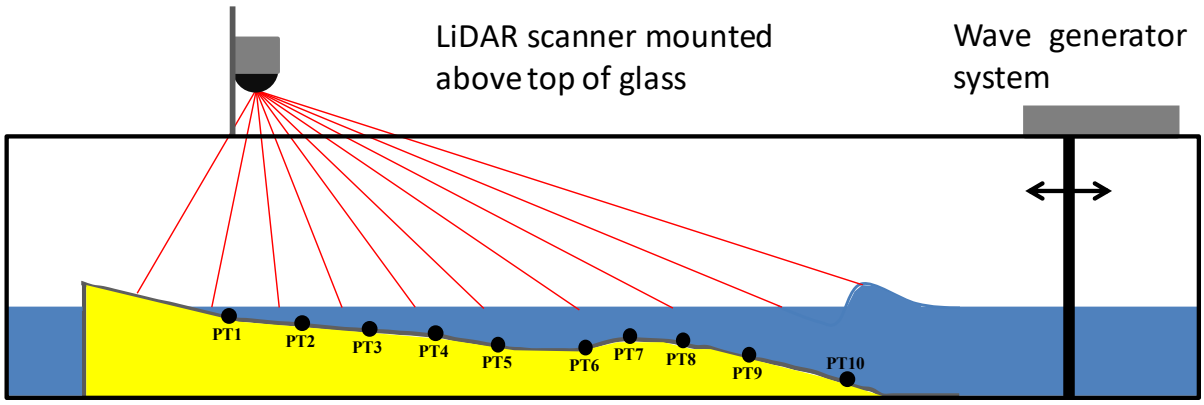

Figure 1 Wave flume setup diagram

Figure 2 Aerial photograph of Tweed Heads and Point Danger at the Queensland/New South Wales border. The fieldwork location at the Tweed River Entrance Sand Bypassing jetty is indicated

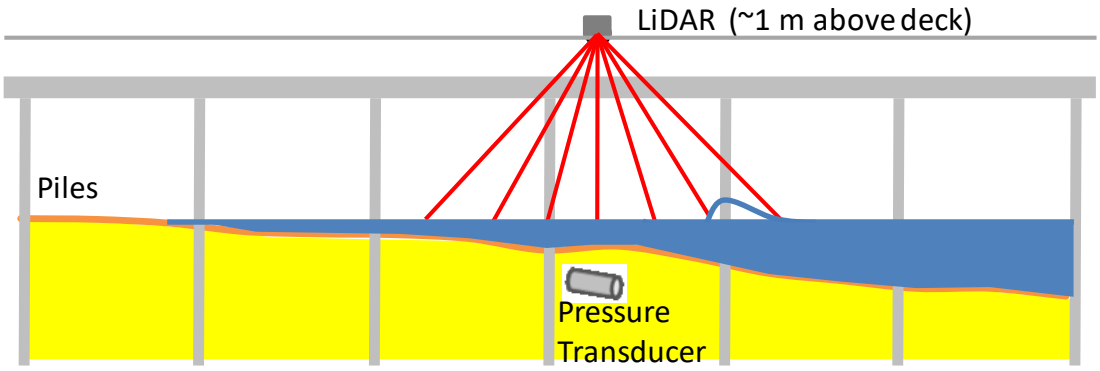

Figure 3 Generalised schematic for surf zone measurements from elevated jetty

Figure 4 Photograph showing the support arm for the overhanging LiDAR at the Tweed jetty. The pressure transducer is located directly beneath this point

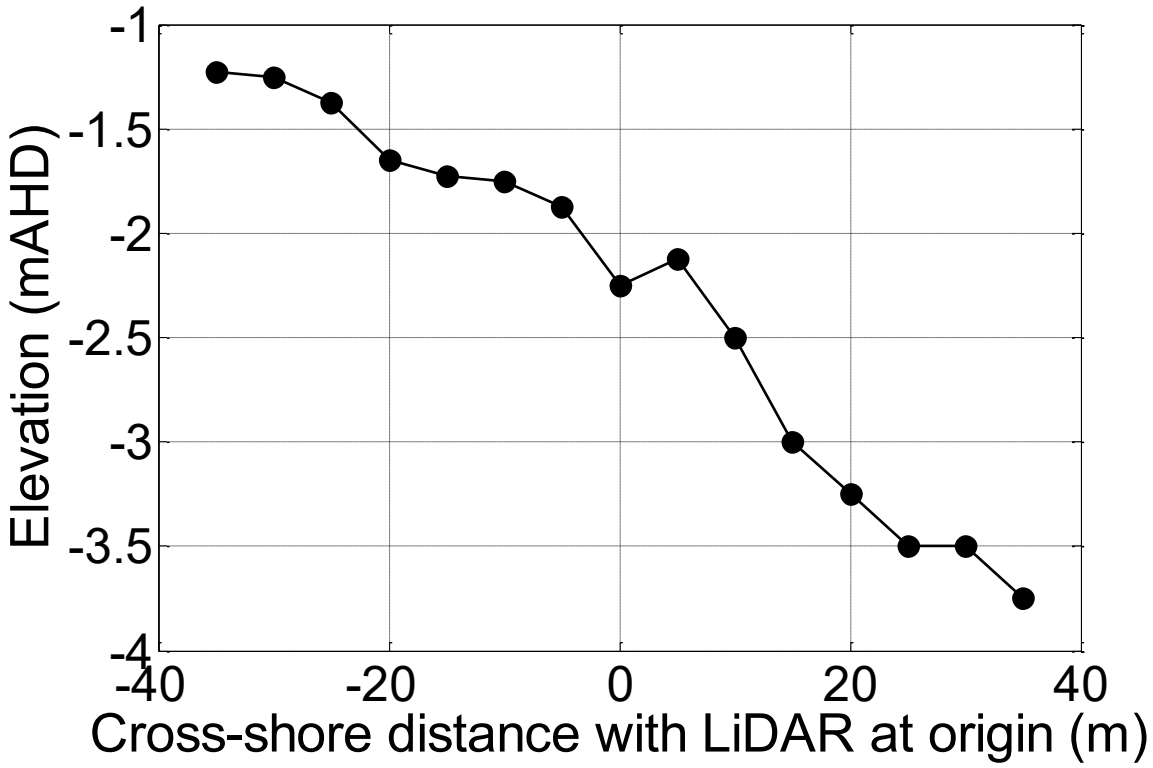

Figure 5 Bathymetry at the Tweed jetty during fieldwork, points indicate depth measurements

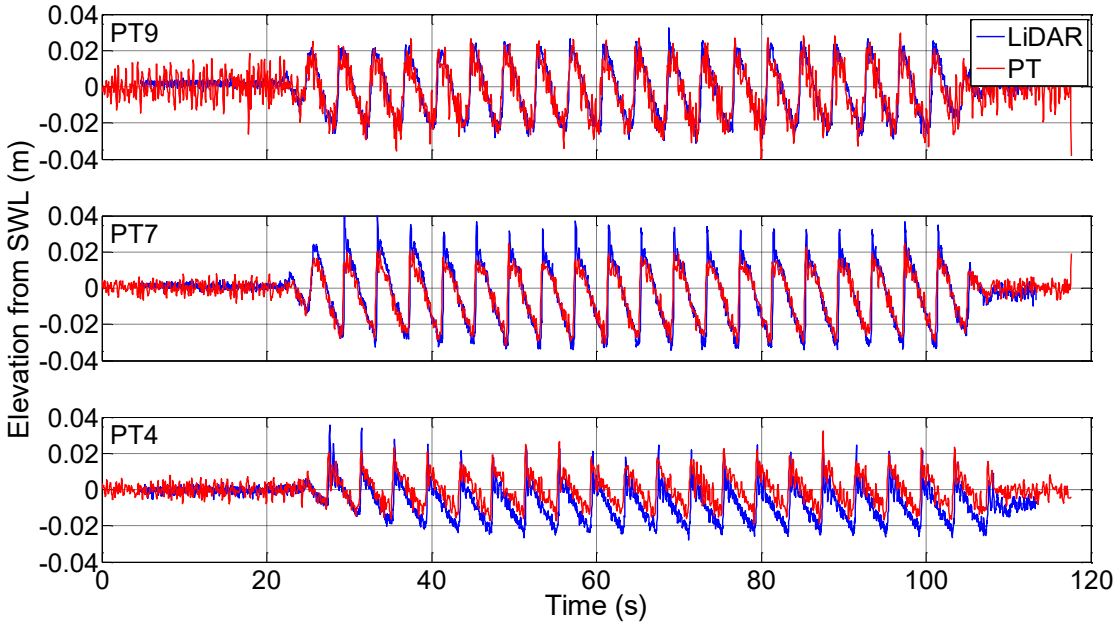

Figure 6 Comparison between LiDAR (black line) and pressure transducer (red line) data at 3 locations along the flume prior to temporal interpolation

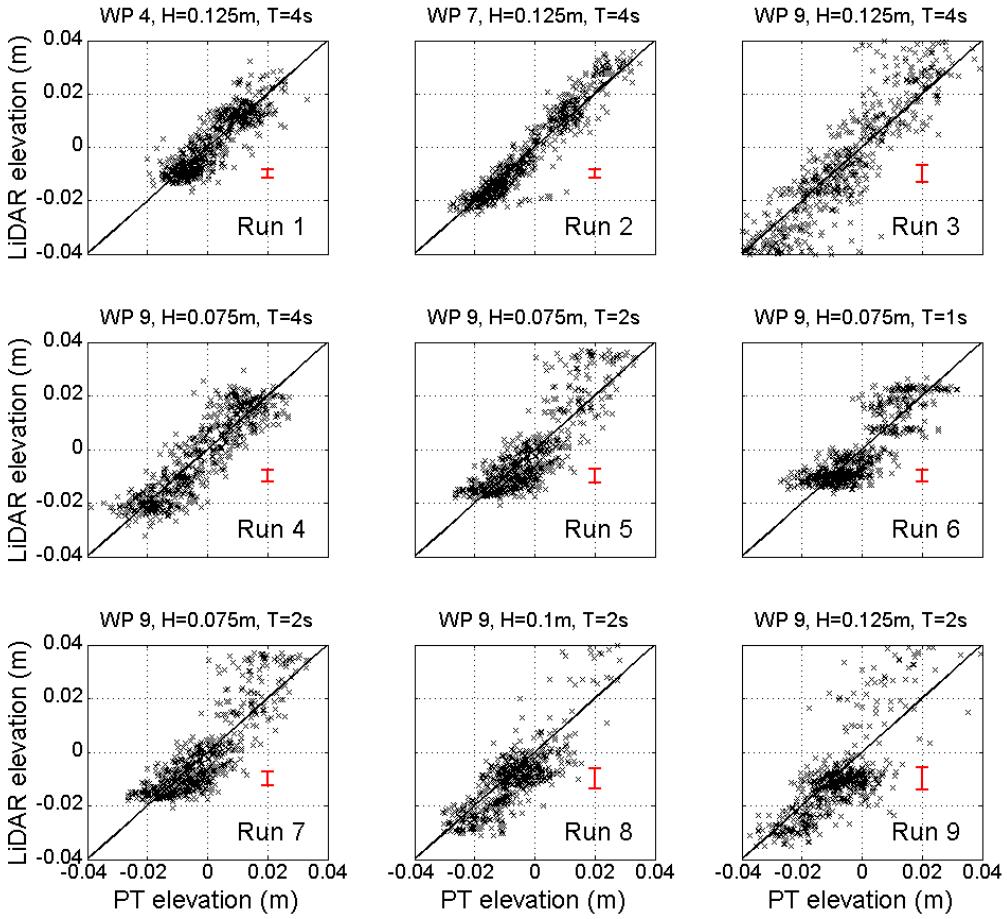

Figure 7 Scatter plot of LiDAR against pressure transducer measurements for various wave height, wave period and PT numbers. Error bars indicate one standard deviation. Details can be found in Table 2

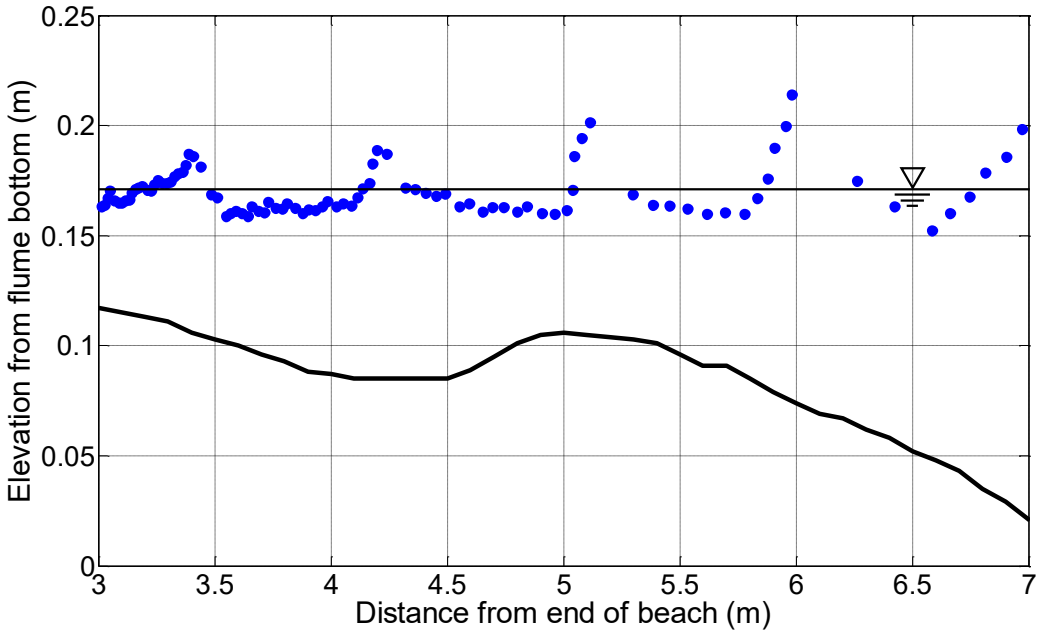

Figure 8 Shadowing is apparent on the lee side of propagating waves and depends on the wave steepness and height of the LiDAR relative to the mean water level

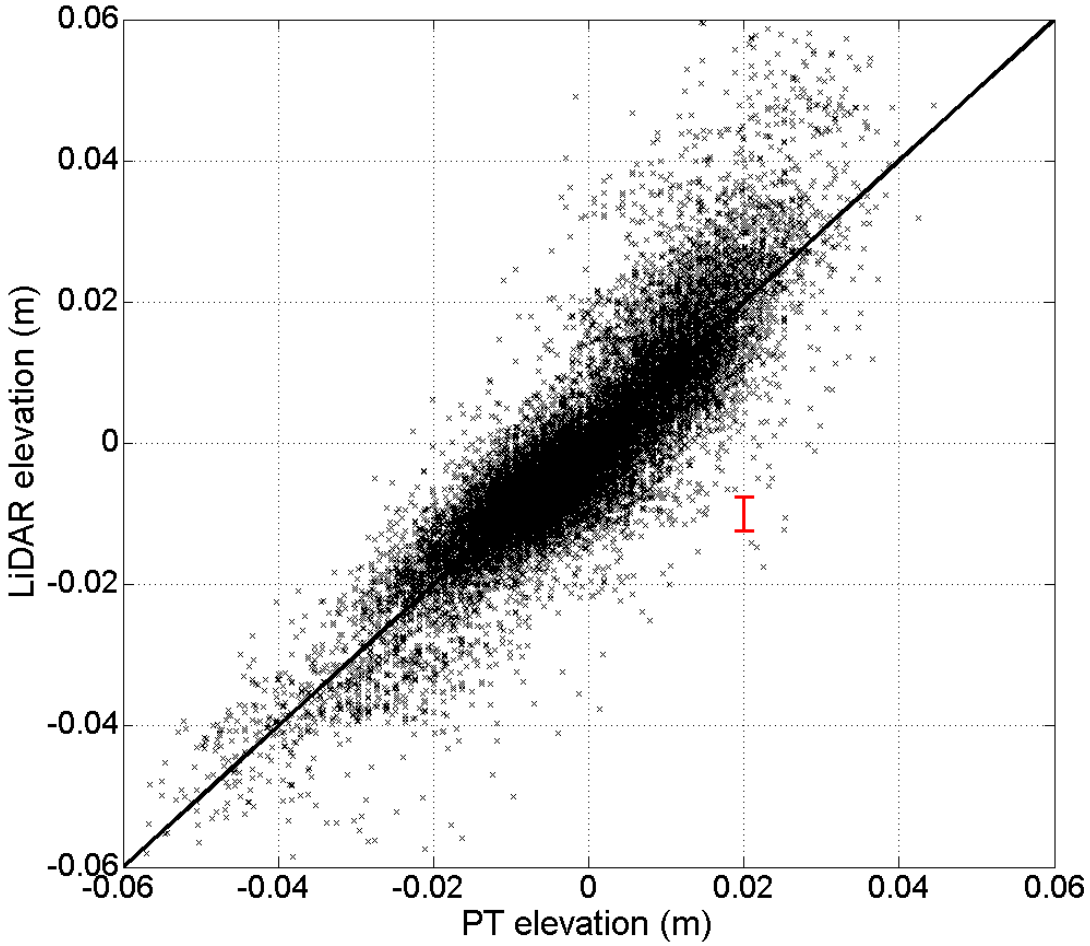

Figure 9 Scatter plot of all pressure transducer and LiDAR measurements for all wave parameters at a fixed water level. One minute of data is included from each run. The error bar indicates one standard deviation

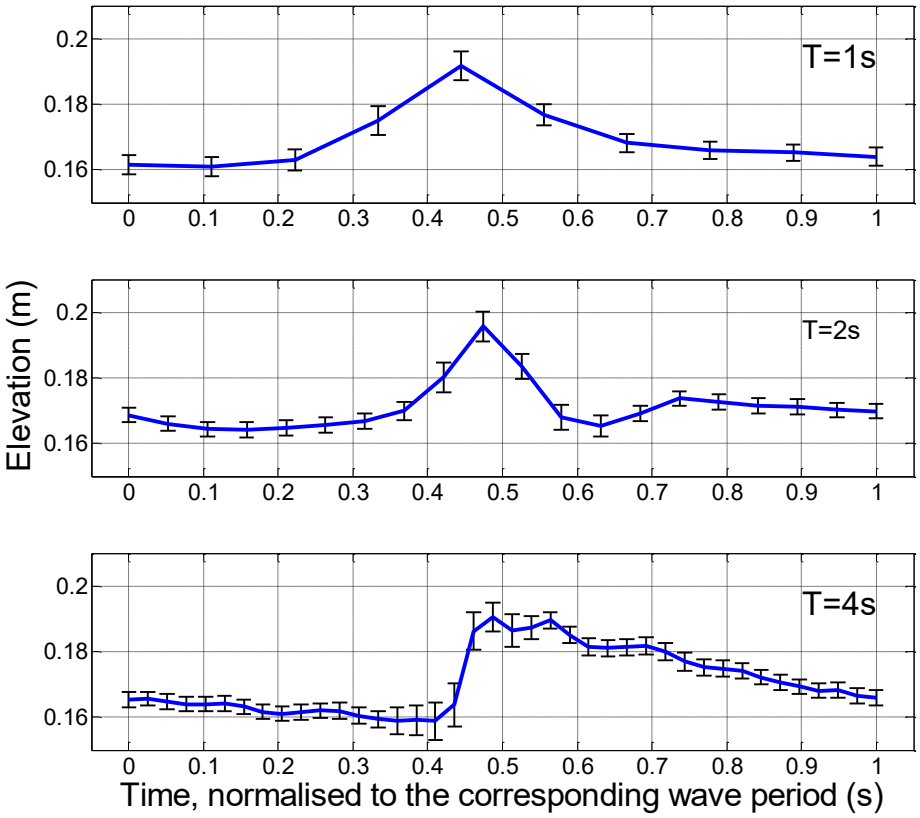

1

2 Figure 10 Normalised time series data for three wave periods. A general baseline (blue line) time series
3 is overlain with the standard deviation error (black bars) between LiDAR and PT for all waves with the
4 corresponding wave period. The error is greatest at the

5

6

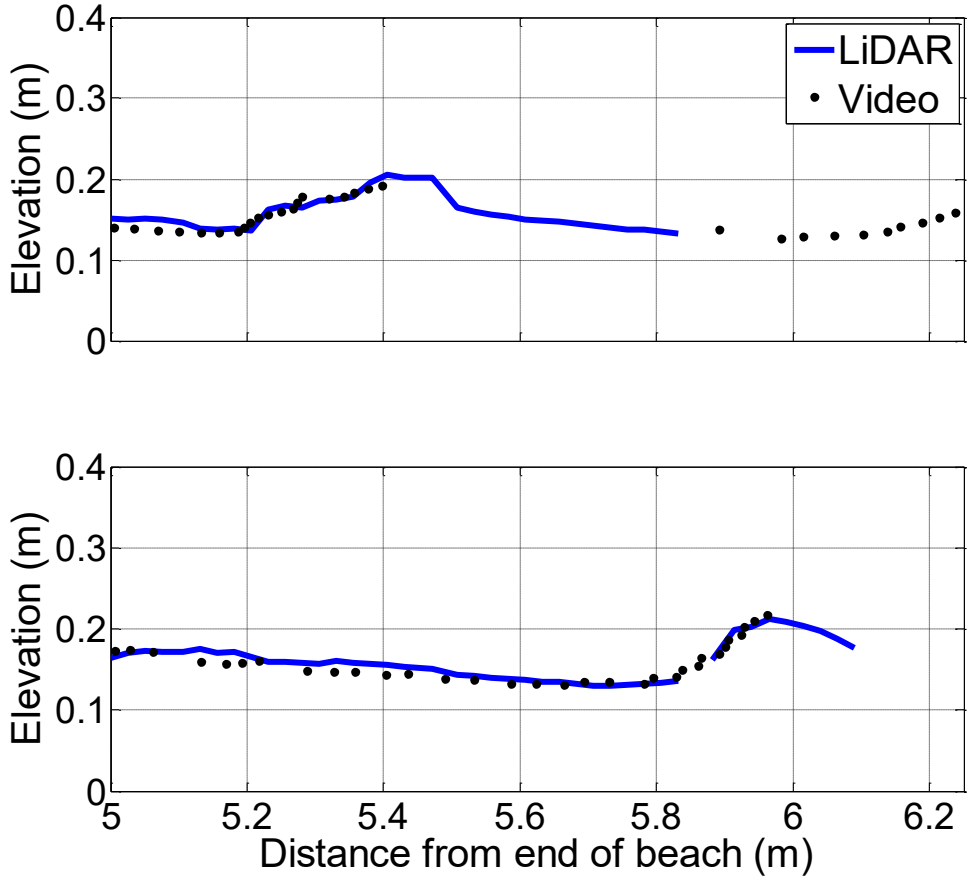

Figure 11 Hi-speed video and LiDAR measurement comparison. Two profiles were selected with the upper plot showing a post-breaking profile and the lower plot showing a pre-breaking profile

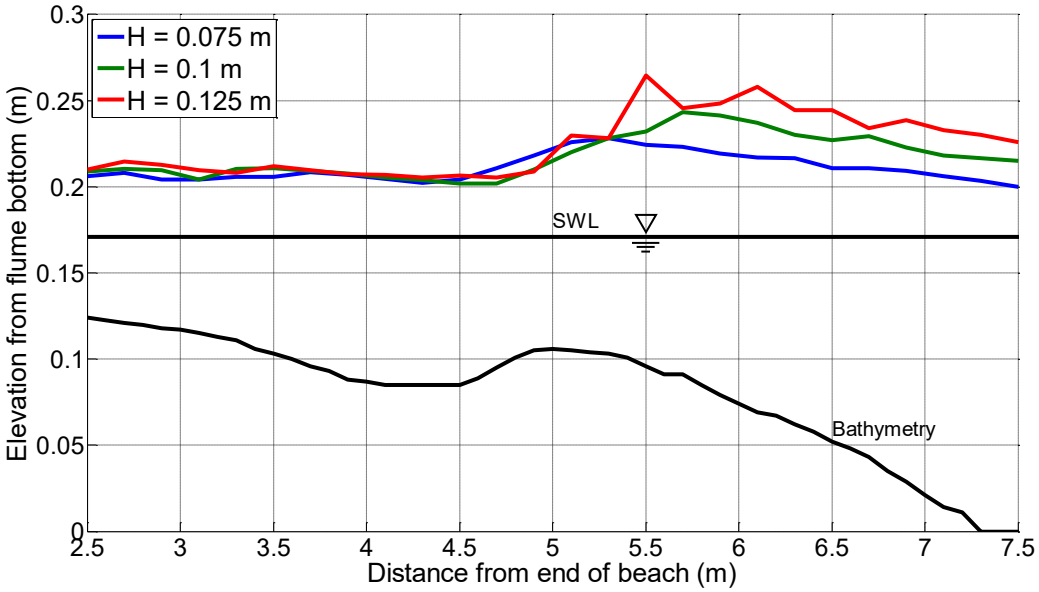

Figure 12 The maximum water elevations across the study domain for three runs with different initial wave heights.

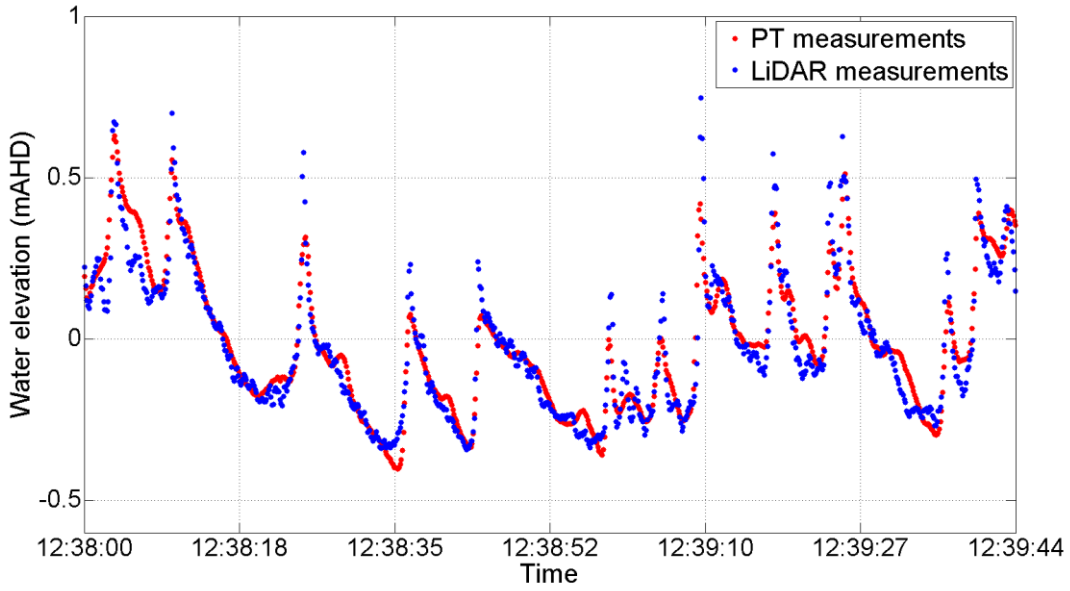

Figure 13 A time series comparison between the LiDAR and pressure transducer measurements at a position directly below the LiDAR

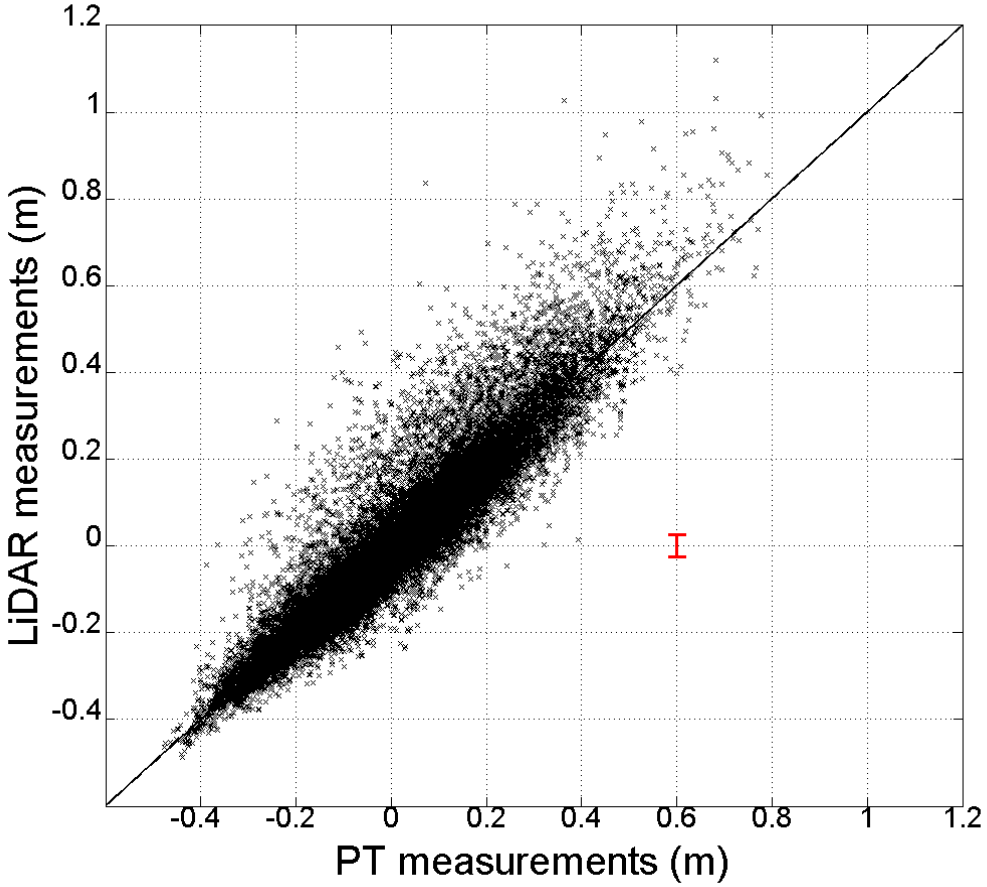

Figure 14 Scatter plot of all pressure transducer and LiDAR measurements at a position directly below the LiDAR for a period over 1h 40mins. The error bar indicates one standard deviation

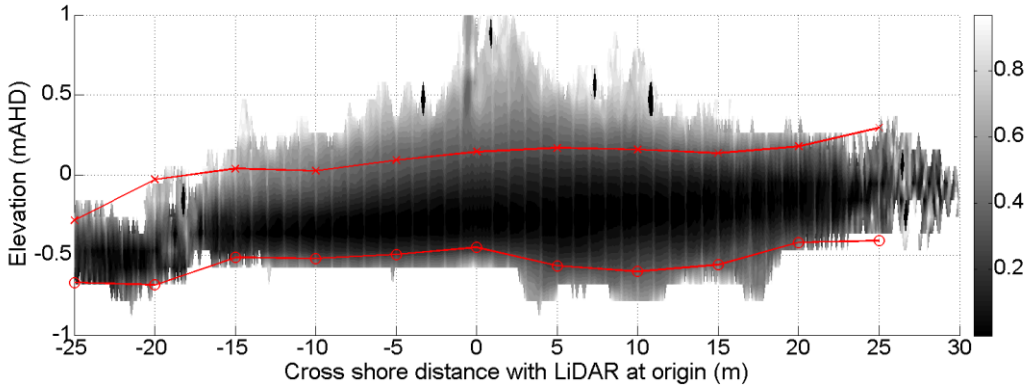

Figure 15 Normalised data point density plot of LiDAR measurements over a period of 30 mins. Profiles for 1% and 99% passing (red line with cross and circles respectively) indicate the maximum wave crest and the minimum trough observed